DOI: 10.5797/jnet.oa.2017-0088

Original Article

Hemodynamic Assessment of Cerebral Aneurysms Using Computational Fluid Dynamics (CFD) Involving the Establishment of Non-Newtonian Fluid Properties

Katsuhiro Tanaka,[1] Fujimaro Ishida,[1] Kimito Kawamura,[2] Hideki Yamamoto,[3] Daiki Horikawa,[3] Tomoyuki Kishimoto,[1] Masanori Tsuji,[4] Hiroshi Tanemura,[5] and Shinichi Shimosaka[1]

Objective: The hemodynamics of cerebral aneurysms was evaluated by computational fluid dynamics (CFD) analysis using the non-Newtonian (Casson's) fluid model and the Newtonian fluid model obtained from measurements. The two fluid models were examined to clarify the influence of blood viscosity on hemodynamic parameters.

Methods: We measured blood viscosity of blood obtained from 50 healthy adults at 12 shear rate ranges using a compact-sized falling needle rheometer. Blood viscosity was set as the Newtonian and Casson's fluid models determined using these measurements. In all, 12 cerebral aneurysms were evaluated by transient analysis to calculate the wall shear stress (WSS), wall shear stress gradient (WSSG), flow velocity (FV), oscillatory shear index (OSI), and parameters that facilitate the quantitative assessment of the fluctuations of individual vectors, including the gradient oscillatory number (GON) and oscillatory velocity index (OVI). Bland–Altman analysis was performed to compare the two models, and systematic errors were examined.

Results: The relationship between the apparent viscosity and the shear rate obtained from blood samples of 50 healthy adults revealed the characteristics of Casson's fluid. The systematic errors in hemodynamic parameters for the two fluid models were small, and the correlation coefficients of the WSS, WSSG, FV, OSI, GON, and OVI were 0.9999, 0.9999, 0.9985, 0.9734, 0.9758, and 0.9258, respectively. Furthermore, the means of these hemodynamic parameters for the entire aneurysm showed a high consistency rate between the two groups, whereas different values were observed in focal hemodynamics including blebs.

Conclusion: Newtonian fluid numerical modeling may be useful for analyzing the entire aneurysm. On the other hand, these results indicated that hemodynamics analyzed using non-Newtonian blood viscosity could have certain effects on focal hemodynamics that may be related to aneurysm growth and rupture.

Keywords ▶ cerebral aneurysm, blood viscosity, computational fluid dynamics, non-Newton fluid

[1]*Department of Neurosurgery, NHO Mie Chuo Medical Center, Hisai, Mie, Japan*
[2]*Asahi Group Holdings, Ltd., Tokyo, Japan*
[3]*Faculty of Environmental and Urban Engineering, Kansai University, Suita, Osaka, Japan*
[4]*Department of Internal Medicine, Kinan Hospital, Minamimuro, Mie, Japan*
[5]*Department of Neurosurgery, Ise Red Cross Hospital, Ise, Mie, Japan*

Received: July 31, 2017; Accepted: February 13, 2018

Corresponding author: Katsuhiro Tanaka. Department of Neurosurgery, NHO Mie Chuo Medical Center, 2158-5 Myojin-Cho, Hisai, 514-1101, Mie, Japan
Email: ghost030303@yahoo.co.jp

The abstract of this study was presented at the 32nd meeting of the Japanese Society for Neuroendovascular Therapy (JSNET 2016).

Introduction

Hemodynamic assessment of cerebral aneurysms using computational fluid dynamics (CFD) facilitates the understanding of the development/enlargement/rupture status of cerebral aneurysms and the risk of rupture. Recently, CFD has been clinically applied to evaluate the rupture point, hemostasis pattern, and course after flow alteration treatment and coil embolization.[1–6)]

Hemodynamic assessment of cerebral aneurysms involves computational science based on numerical modeling of blood flow/boundary conditions/blood using patient-specific geometry. Establishing patient-specific data in blood or boundary conditions is difficult. For this reason, in many studies involving a large number of patients, standardized values of blood flow volume at an inlet, blood density, and blood viscosity were adopted.

In many studies, blood was assumed to be a Newtonian fluid with a constant blood viscosity. However, blood is a non-Newtonian fluid, and blood viscosity increases in a low shear rate range, whereas it is constant in a high shear rate range. The non-Newtonian properties of blood have been expressed using structural formulae, such as the Casson, Herschel–Bulkley, and Carreau–Yasuda models. Furthermore, the shear rate is reduced in a portion of the aneurysm site, and changes in viscosity may be involved in intraaneurysmal thrombosis or aneurysmal wall remodeling.[2,7)] Therefore, accurate numerical modeling of blood viscosity, which changes in accordance with the shear rate, may contribute to the optimization of hemodynamic assessment. In this study, we measured blood viscosity in a wide shear rate range using a compact-sized falling needle rheometer, and prepared shear rate–apparent blood viscosity curves for healthy adults. In addition, we performed CFD analysis of cerebral aneurysms using patient-specific geometry, and compared Newtonian model, in which blood viscosity is constant, with Casson's model, in which shear rate–apparent blood viscosity curves obtained in healthy adults were established, to examine the influence of blood viscosity on hemodynamic parameters.

Subjects and Methods

Measurement of blood viscosity

The subjects were 50 healthy adults (5 males and 5 females per age group (20–29, 30–39, 40–49, 50–59, and 60–69 years). Blood was collected between 7:30 and 8:00 a.m. after fasting without restrictions regarding water intake. Those with a history of cerebrovascular disorder, coronary artery disease, obstructive arteriosclerosis, or malignant tumors and those receiving antithrombotic drugs were excluded. The protocol of this clinical study was approved by the Ethics Review Board of our hospital (Approval number: 2016-09).

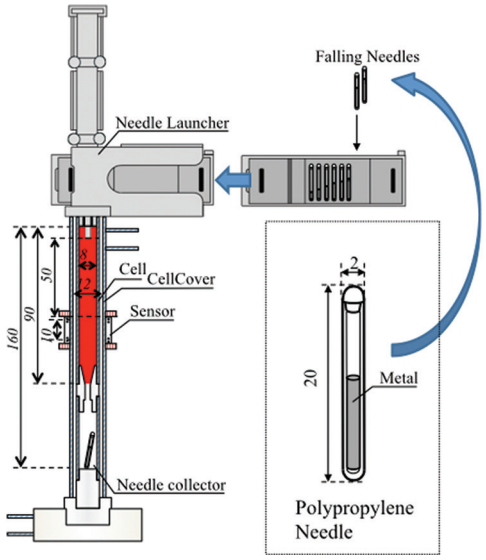

Fig. 1 Schematic of a compact-sized falling needle rheometer.

After blood collection, all syringes were kept warm by incubating in a thermostatic water tank at 37°C for 10 minutes, and blood was then placed in the measuring cell of a compact-sized falling needle rheometer (Asahi Group Holdings, Ltd., Tokyo, Japan, Nippon Steel & Sumikin Technology Co., Ltd., Tokyo, Japan) (**Fig. 1**). The sample temperatures were reduced due to temperature differences from the laboratory room or rheometer. Our previous study confirmed that the mean temperature was 32°C. Measuring container surface is made of polypropylene and plastic syringes for blood collection were used: plastic EDTA-2K, 6 cc (BD Vacutainer blood collection tubes; Japan Becton, Dickinson Co., Ltd., Tokyo, Japan). The measuring cell of the rheometer was made of polypropylene. For all subjects, the interval from blood collection until viscosity measurement was within 2 hours. For fluid analysis, 12 needles of the same shape but different sinker and different mean density were allowed to fall freely into the blood-containing measuring cell of a rheometer at a terminal rate. **Figure 2** shows the fluid model around the needle free-falling at the terminal speed. Relation between shear stress (τ) and shear rate (γ) of human blood were calculated using the following balance equations, that is, the momentum balance around the falling needle; force balance acting on minute circular cylindrical core around the falling needle; and fluid

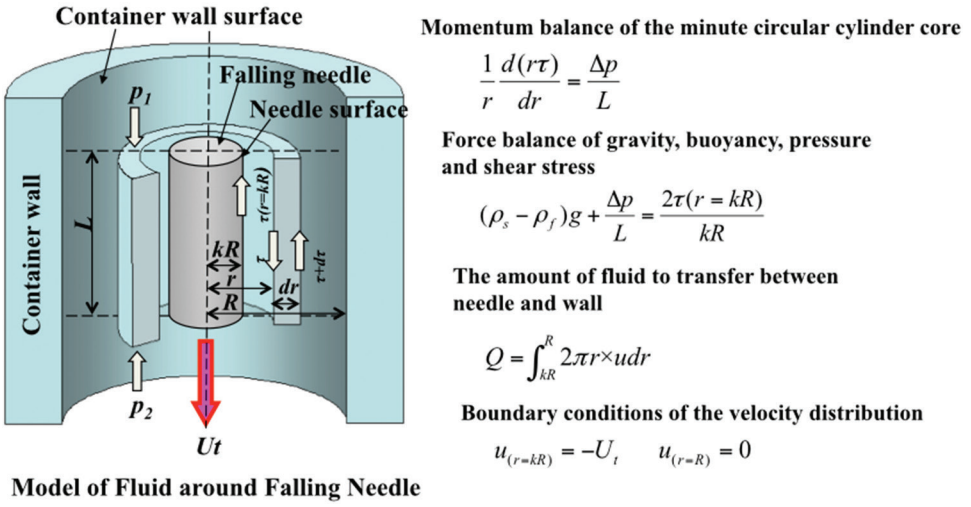

Fig. 2 Fluid model around needles falling freely at a terminal velocity and various balance formulae.

amount to transfer between the falling needle surface and the container wall under the boundary conditions (**Fig. 2**).[8] Blood density was measured using a portable density meter (DMA-35; Anton Paar Co., Ltd., Graz, Austria) (accuracy of measurement: 10^{-3} g/cm^{-3}, reproducibility: 5×10^{-4} g/cm^{-3}). Measuring cells to be re-used were washed in water and immersed in lavage fluid to remove protein stains. Subsequently, ultrasonic cleaning was performed. As lavage fluid, Endozime AW Triple Plus (RUHOF Corp., NY, USA) was diluted 1:20 before use. After washing, the measuring cells were sufficiently washed in water and dried. We calculated the apparent viscosity at 12 shear rate ranges by substituting measurements for the above formulae. Based on this, we prepared a shear rate–apparent blood viscosity curve and applied it to the Casson's model. On the other hand, blood functions as a Newtonian fluid in a high shear rate range, and we approximately calculated the viscosity in a sufficiently high shear rate range (3000 s^{-1}) on the above blood viscosity curve and applied it to the Newtonian model.

CFD analysis of cerebral aneurysms

Patient-specific geometry models

In all, 12 internal carotid artery aneurysms were included in this study (**Fig. 3**). The Digital Imaging and COmmunication in Medicine (DICOM) data obtained with 3D-CTA were loaded into Mimics Innovation Suite 16.0 (Materialise Japan, Kanagawa, Japan), and segmentation of the geometry was conducted. The data were output as stereolithography (STL). The STL file was integrated into Magics 17.01 (Materialise Japan), and a blood vessel in the region of interest was extracted. To correct the distortion of a triangle comprising STL, it was remeshed with a triangle measuring 0.25 mm at the maximum length using 3-matic 8.0 (Materialise Japan). In addition, curvature smoothing was performed to prepare a patient-specific geometry model.

Mesh generation

The patient-specific geometry model was integrated into ANSYS ICEM 16.1 (ANSYS Inc., Canonsburg, PA, USA), and the tetrahedral element was established as 0.6 mm at maximum and 0.1 mm at minimum using Octree's method. Subsequently, curvature refinement was performed. On the vascular surface, six-layer prism elements were added, with initial and total heights of 0.015 mm and 0.148 mm, respectively. To establish fully developed laminar flow at an inlet, the inlet length was calculated according to Poiseuille's law, and the blood vessel was prolonged vertically to the inlet surface.

Numerical modeling

For the fluid domain, 3D incompressible laminar flow fields were obtained by solving the continuity and Navier–Stokes equations, and discretization was performed using the finite volume method. The blood density was 1056 kg/m^3, and its viscosity in the Newtonian model was 0.0057 Pa·s. In Casson's model, a shear rate–apparent blood viscosity curve was established, and transient analysis was conducted using ANSYS CFX 16.1 (ANSYS Inc.). Traction-free boundary conditions were applied at outlets. At an inlet, the blood flow volume was established in accordance with the inner vascular diameter based on the mass flow waveform of the internal carotid artery in healthy adults. Assuming that the blood flow volume may be proportional to the cube

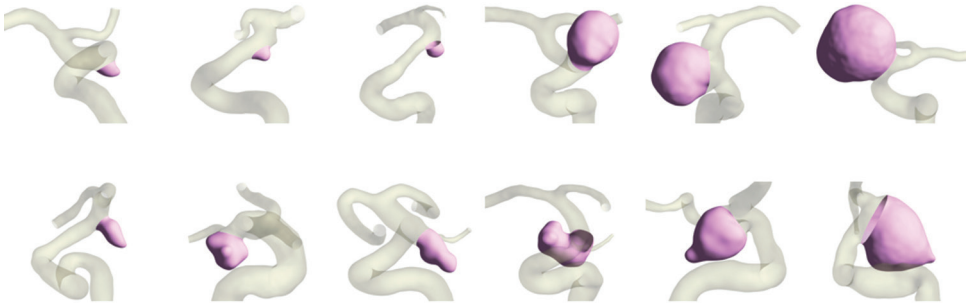

Fig. 3 Twelve aneurysms of the internal carotid artery. The upper row indicates six cases of unruptured aneurysms, and the lower row indicates six cases of ruptured aneurysms.

of the vascular lumen diameter based on Poiseuille's law (following formula), and that the minimum-cost-hypothesis-based constant shear theory may be achieved under physiological conditions, the wall shear stress (WSS) was established as 1.5 Pa for calculation.[9,10] As hemodynamic parameters, we measured the WSS, wall shear stress gradient (WSSG), flow velocity (FV), and oscillatory shear index (OSI). In addition, the hemodynamic parameters that represent the fluctuations of vectors of WSSG and FV, gradient oscillatory number (GON), and oscillatory velocity index (OVI)[11] were calculated. For statistical analysis, JMP 9 software (SAS Institute Inc., Cary, NC, USA) was used. Bland–Altman analysis of morphological and hemodynamic parameters for the Newtonian and Casson's models was conducted. The systematic error and correlation coefficient were calculated and examined.

Poiseuille's solution, which relates the vessel flow rate, Q, blood viscosity, μ, vessel diameter, d, and WSS, τ_w, is shown below.

$$Q = \frac{\pi}{32\mu}\tau_w d^3$$

Hemodynamic parameters

WSS

Wall shear stress was calculated as the mean time integration over the cardiac cycle.

$$\mathrm{WSS} = \frac{1}{T}\int_0^T |\,\mathrm{wss}_i\,|\,dt$$

where wss_i is the instantaneous WSS vector and T is the duration of the cycle.

OSI

Oscillatory shear index is an index that is used to evaluate the fluctuation of the WSS vector, regarding the time direction average value per heart beat for the WSS vector as a reference. Oscillatory shear index is calculated using the following formula. A high OSI value is consistent with thickening of the vascular intima at the bifurcation of the carotid artery. Furthermore, a study reported the association between this index and arteriosclerosis of the cerebral aneurysm wall.

$$\mathrm{OSI} = \frac{1}{2}\left(1 - \frac{\left|\int_0^T \mathrm{wss}_i\,dt\right|}{\int_0^T |\,\mathrm{wss}_i\,|\,dt}\right)$$

where wss_i is the instantaneous WSS vector and T is the duration of the cycle.

WSSG

To examine the uniformity of WSS distributions in the WSS vector direction on transient analysis, we evaluated the WSSG. When disintegrating the WSS vector in the contact surface direction into WSS time average vector (p) and vertical (q) directions on the contact surface, this index is calculated using the following formula. The WSSG is correlated with the degree of turbulence and is involved in the activation of local atherosclerosis.

$$\mathrm{WSSG} = \sqrt{\left(\frac{\partial \tau_{w,p}}{\partial p}\right)^2} + \sqrt{\left(\frac{\partial \tau_{w,q}}{\partial q}\right)^2}$$

where τ_w is the WSS vector, the p-direction corresponds to the time-averaged direction of the WSS, and the q-direction is perpendicular to p.

GON

This index is used to evaluate the fluctuation of the WSSG vector. The GON resembles the relationship between the WSS vector and OSI and is calculated using the following

Table 1 Patient background

Sex		Male	Female	All
		25	25	50
Age: 20–29 years		5	5	10
Age: 30–39 years		5	5	10
Age: 40–49 years		5	5	10
Age: 50–59 years		5	5	10
Age: 60–69 years		5	5	10
Age mean		43.6	43.9	43.7
BMI mean		23.1	21.1	22.1
Smoke	Never (%)	18 (72)	21 (84)	39 (78)
	Former (%)	4 (16)	2 (8)	6 (12)
	Current (%)	3 (12)	2 (8)	5 (10)
Drink	Never (%)	14 (56)	22 (88)	36 (72)
	Current (%)	11 (44)	3 (12)	14 (28)
Hypertension (%)		2 (8)	2 (8)	4 (8)
Diabetes mellitus (%)		1 (4)	0 (0)	1 (2)
Dislipidemia (%)		4 (16)	3 (12)	7 (14)

BMI: Body Mass Index

formula. The GON was developed to explain the development of cerebral aneurysms. The development of side-wall (or lateral)-type cerebral aneurysms at sites with a high GON was confirmed.

$$\mathrm{GON} = 1 - \frac{\left| \int_0^T \mathrm{wssg}_i \, dt \right|}{\int_0^T |\mathrm{wssg}_i| \, dt}$$

where wssg_i is the instantaneous WSS gradient vector and T is the duration of the cycle.

FV

In the blood flow area, we calculated the time average FV (m/s) and evaluated the FV vector on 3D streamlines or arbitrary cross sections.

OVI

The time-dependent fluctuation of the FV vector in the blood flow area was calculated using the following formula. The FV in complex-shaped aneurysms may decrease, increasing the time-dependent vector fluctuation. We reviewed the results of assessment in the state of rupture. In patients with ruptured cerebral aneurysms, the OVI is higher than in those with unruptured cerebral aneurysms.[11)]

$$\mathrm{OVI} = \frac{1}{2}\left(1 - \frac{\left| \int_0^T \mathrm{fv}_i \, dt \right|}{\int_0^T |\mathrm{fv}_i| \, dt} \right)$$

where fv_i is the instantaneous FV vector and T is the duration of the cycle.

Results

Measurement of blood viscosity

The background of the 50 subjects (healthy adults) is shown in **Table 1**. As blood viscosity, the properties of non-Newtonian fluid approximated using Casson's formula (shown below) are presented. The average shear rate–apparent blood viscosity curves were made based on the actual values of apparent blood viscosity obtained at 12 shear rate ranges (**Fig. 4A**). We prepared average approximate curves for all subjects, males, and females (**Fig. 4B**). The apparent viscosity in males was slightly higher than in females. In this study, the average shear rate–apparent blood viscosity curve in the subjects was applied to Casson's model for CFD analysis. On the other hand, the blood viscosity at a shear rate of 3000 1/s on this average curve was 0.0057 Pa·s, which was regarded as the blood viscosity of the Newtonian model.

$$\sqrt{\tau} = \sqrt{\tau_0} + \sqrt{\eta\gamma}$$

Casson's equation, which relates shear stress, τ, yield stress, τ_0, viscosity, η, and shear rate, γ, is shown above.

CFD analysis of aneurysms

In all, 12 patients with internal carotid artery aneurysms included six with unruptured cerebral aneurysms (mean aneurysmal height: 7.9 ± 5.5 mm, mean neck width: 6.9 ± 3.5 mm) and six with ruptured cerebral aneurysms (mean aneurysmal height: 8.0 ± 3.2 mm, mean neck width: 5.9 ± 3.0 mm). We calculated hemodynamic parameters for all aneurysms using the Newtonian and Casson's models in the 12 patients, performed Bland–Altman analysis, and

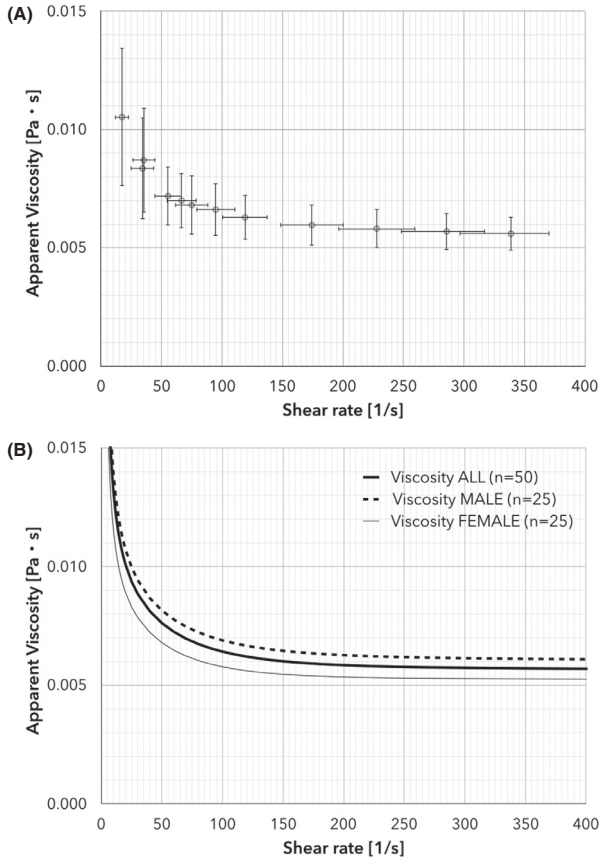

Fig. 4 (**A**) The horizontal axis represents the shear rate (1/s) in 50 healthy adults. The vertical axis represents the apparent blood viscosity (Pa·s). The small circles represent the mean apparent viscosity in each shear rate range measured using 12 falling needles at 32°C. The horizontal bars represent the shear rate, and the vertical bars represent the 95% confidence interval of apparent viscosity. (**B**) The average apparent viscosity curves prepared by manual fitting are presented. The broken line represents the average curve for 25 males, the thick solid line represents that for all 50 subjects, and the thin solid line represents that for 25 females.

calculated the bias between the two models. The bias 95% confidence interval (CI) and correlation coefficient (r) were as follows: WSS: bias = -4.41×10^{-3} Pa, bias 95% CI = $-1.32\ 10^{-2}$ to 4.41×10^{-3} Pa, $r = 0.9999$; OSI: bias = 6.52×10^{-4}, bias 95% CI = -7.51×10^{-4} to 2.05×10^{-3}, $r = 0.9734$; WSSG: bias = −16.8 Pa/m, bias 95% CI = −25.5 to −8.07 Pa/m, $r = 0.9999$; GON: bias = 6.60×10^{-4}, bias 95% CI = -1.84×10^{-3} to 3.16×10^{-3}, $r = 0.9758$; FV: bias = -2.64×10^{-3} m/s, bias 95% CI = $-5.85\ 10^{-3}$ to 5.61×10^{-4} m/s, $r = 0.9985$; OVI: bias = -1.10×10^{-4}, bias 95% CI = -1.61×10^{-3} to 1.39×10^{-3}, and $r = 0.9258$ (**Fig. 5**). Errors in the parameters for all aneurysms between the two models were small, suggesting high consistency (**Fig. 6A**). On the other hand, the FV vector or OVI differed at intra-aneurysmal irregular sites, such as blebs, in one patient with an unruptured aneurysm and two with ruptured aneurysms. A representative case is presented (**Fig. 6B**).

Discussion

Blood viscosity depends on the quality/quantity of blood cell components, quantity of plasma components, interactions between cell and plasma components, and blood flow. Therefore, blood is considered a non-Newtonian fluid, of which the viscosity changes with the shear rate, but not a Newtonian fluid, which has a specific viscosity.[12,13] In particular, several studies reported that an increase in viscosity in a low shear rate range could affect the endothelium of blood vessels, resulting in peripheral artery diseases or ischemic cerebrovascular disorders.[2,14,15] However, in many large-scale studies, blood viscosity was measured in a specific shear rate range.[16] Few studies have examined changes in blood viscosity in a broad shear rate range. In this study, we investigated whether these blood viscosity characteristics influence the hemodynamics by CFD analysis of cerebral aneurysms based on the data obtained from a compact-sized, high-accuracy, and falling needle rheometer[17] (apparent viscosity curve).

We measured the apparent blood viscosity at 12 shear rate ranges in 50 healthy adults and prepared average shear rate–apparent blood viscosity curves. To our knowledge, this is the first average blood viscosity curve in a broad shear rate range. In this study, blood viscosity was consistent with Casson's formula, in which viscosity increases in a low shear-rate range, as previously reported.[12,13] However, neither Casson's yield value nor Casson's viscosity at a shear rate of zero could be calculated due to technical limitations; in this study, we adopted an approximate equation that diverges infinitely at a shear rate of zero. On the other hand, blood acts as a Newtonian fluid in a high shear rate range (>300 1/s); therefore, the blood viscosity (0.0057 Pa·s) in a sufficiently high shear rate range (3000 1/s) on our average viscosity curve was established as the blood viscosity of the Newtonian model. According to previous studies, blood viscosity ranges from 0.003 to 0.004 Pa·s. A dissociation was found between our results and previous studies. However, the results of our previous pilot study showed that the viscosity of samples stored at 37°C was 10%–20% lower than when samples were stored at 32°C, suggesting that viscosity depends on the temperature of the measurement environment.

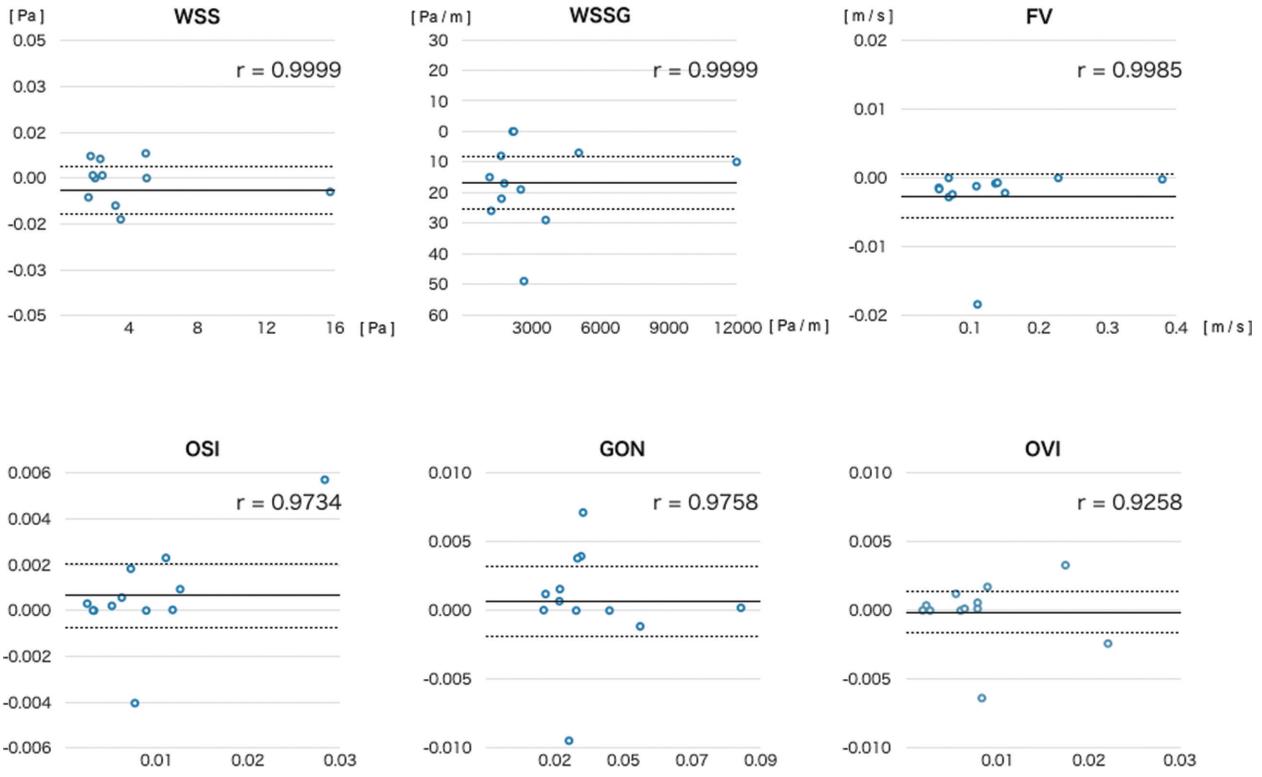

Fig. 5 The results of Bland–Altman analysis of hemodynamic parameters using the Newtonian and Casson's models in 12 internal carotid artery aneurysms are shown. The horizontal axis shows the mean value of each parameter in the Casson's and Newtonian models. The vertical axis shows differences in the values between the two models. The solid lines represent the bias. The dotted lines represent the bias 95% confidence interval. *r* is the correlation coefficient. The WSS (upper left), WSSG (upper middle), and FV (upper right) showed a high consistency between the two models. The OSI (lower left), GON (lower middle), and OVI (lower right) showed slightly lower values. FV: flow velocity; GON: gradient oscillatory number; OSI: oscillatory shear index; OVI: oscillatory velocity index; WSS: wall shear stress; WSSG: wall shear stress gradient

CFD analysis using Casson's model

Ohta et al.[18] applied the dynamic viscosity of non-Newtonian fluid for the simulation of hemodynamics after stenting for cerebral aneurysms and speculated that a rapid decrease in WSS and an increase in viscosity in the aneurysm after stenting may lead to intra-aneurysmal thrombus formation. Xiang et al.[19] reported a reduction in WSS at the aneurysmal bleb by CFD analysis with Casson's model in comparison with the Newtonian model, suggesting that the risk of aneurysmal rupture may be underestimated by Newtonian model calculation. Suzuki et al.[20] applied two models, Casson's and Newtonian models, which differ in viscosity, for CFD analysis of unruptured cerebral aneurysms, and reported that the normalized WSS was reduced by 25% at maximum in Casson's model, suggesting the influence of viscosity on CFD analysis. In this study, we prepared Casson's model from the average shear rate–blood viscosity curve based on the actual values of 50 healthy adults, and applied it for CFD analysis for the first time. As a result, among the hemodynamic parameters, we found no apparent differences in the mean WSS, WSSG, or FV between the two models, and we found no involvement of the aneurysm size or presence or absence of rupture. The correlation coefficients of the OSI, GON, and OVI, which represent the fluctuations of the vectors of the above three parameters, were slightly reduced. In particular, we observed some patients with ruptured/unruptured aneurysms in whom the FV vector differed at focal irregular zones such as blebs. These results suggest that conventional CFD analysis in which blood is considered a Newtonian fluid is useful for evaluating the physical quantity of the entire aneurysm as a mean, and that the results of hemodynamic prediction may differ in focal irregular zones such as blebs, which play an important role in aneurysmal growth or rupture. In the future, a larger number of patients must be analyzed.

Limitations

Blood viscosity has Casson's yield value on fluid arrest and Casson's viscosity. However, measuring these values is technically difficult, and we used an approximate equation

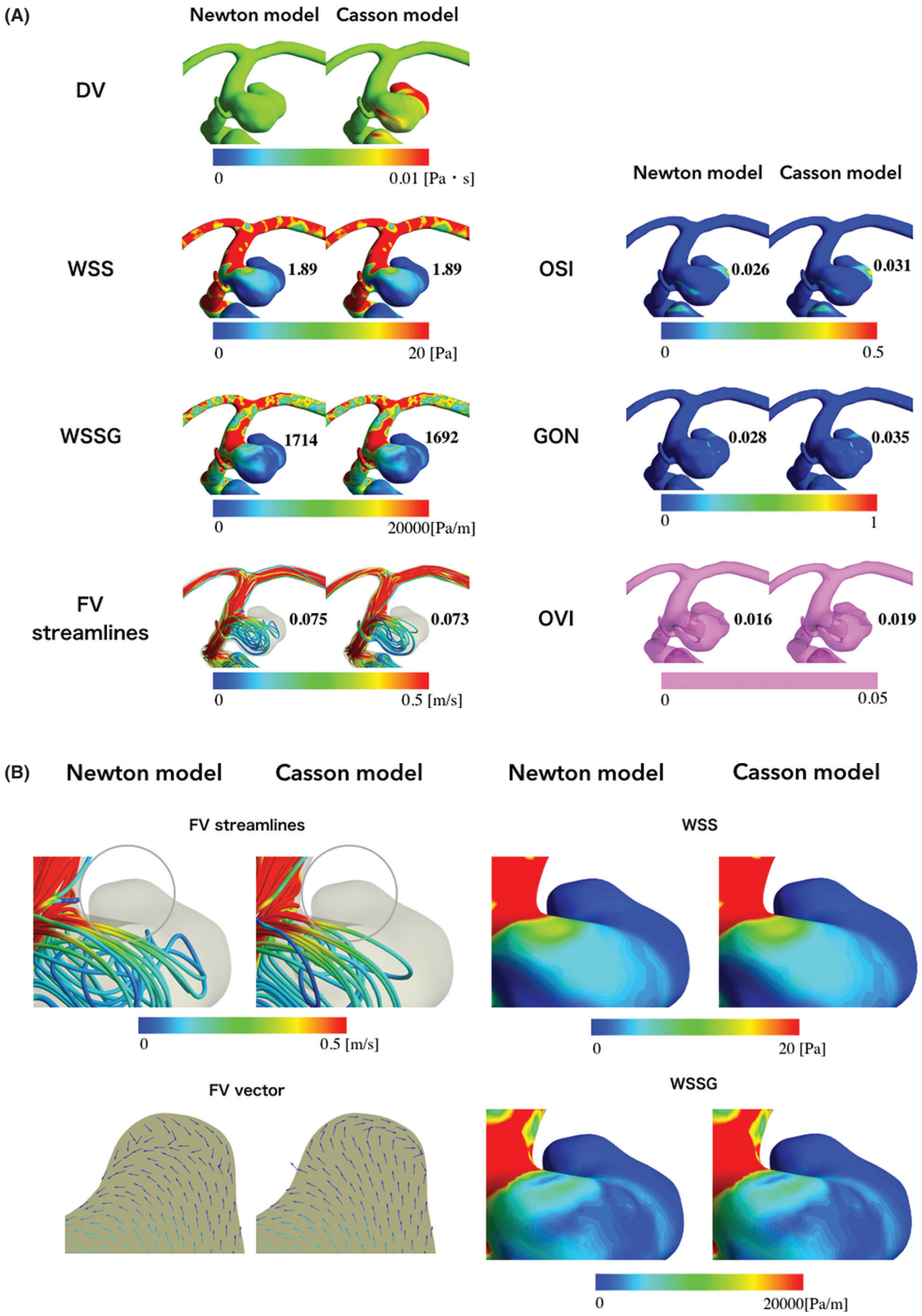

Fig. 6 (**A**) Computational fluid dynamics analysis of an internal carotid artery aneurysm. The viscosity and six representative parameters are illustrated with the mean value of each parameter for the entire aneurysm. (**B**) Magnified images of (**A**). Streamlines were not visualized with blebs (gray circles) (upper left), but different blood flow patterns were observed when evaluating the time average FV vector with blebs (gray circles, lower left). On the other hand, the WSS and WSSG were similar between the two models (upper right, lower right). CDF: computational fluid dynamics; DV: dynamic viscosity; FV: flow velocity; GON: gradient oscillatory number; OSI: oscillatory shear index; OVI: oscillatory velocity index; WSS: wall shear stress; WSSG: wall shear stress gradient

in this study. Physiologically, no infinite viscosity exists at a shear rate of zero, but we did not find an intra-aneurysmal shear rate of zero or an extremely low value in this study; therefore, the calculated results may be quite accurate. Furthermore, approximate curves were prepared by manual fitting. Considering these limitations, we will report mathematically accurate approximate equations.

Despite the preparation of average curves, blood viscosity dynamically changes; therefore, evaluation of a morbid state related to changes in the physical properties of blood or circulatory status is important. In the future, blood viscosity should be measured as patient-specific data in patients with stroke to carry out more accurate hemodynamic simulation.

Lastly, some hemodynamic parameters were different between the two models in a focal irregular zone. However, we could not compare these hemodynamic parameters among the parts of the aneurysm such as the neck, dome, and bleb. Inter-model inconsistency detection for focal hemodynamic parameters was evaluated subjectively. Quantification of hemodynamic parameters with respect to these parts of the aneurysm may be necessary although technically difficult.

Conclusion

Based on the hematological data from 50 healthy adults, we measured blood viscosity at 12 shear rate ranges, and prepared an average shear rate–apparent blood viscosity curve. The results were applied to CFD analysis for cerebral aneurysms, and hemodynamic parameters at local aneurysm sites were compared between Newtonian and Casson's fluid models. CFD analysis in which blood is considered to be a Newtonian fluid is useful for evaluating the physical quantity of the entire aneurysm as a mean, but hemodynamics may differ in focal aneurysm zones such as blebs, suggesting the necessity of considering non-Newtonian properties for optimal analysis.

Disclosure Statement

There is no conflict of interest for the main author and coauthors.

References

1) Cebral JR, Castro MA, Burgess JE, et al: Characterization of cerebral aneurysms for assessing risk of rupture by using patient-specific computational hemodynamics models. *AJNR Am J Neuroradiol* 2005; 26: 2550–2559.
2) Cebral J, Ollikainen E, Chung BJ, et al: Flow conditions in the intracranial aneurysm lumen are associated with inflammation and degenerative changes of the aneurysm wall. *AJNR Am J Neuroradiol* 2017; 38: 119–126.
3) Miura Y, Ishida F, Umeda Y, et al: Low wall shear stress is independently associated with the rupture status of middle cerebral artery aneurysms. *Stroke* 2013; 44: 519–521.
4) Fukazawa K, Ishida F, Umeda Y, et al: Using computational fluid dynamics analysis to characterize local hemodynamic features of middle cerebral artery aneurysm rupture points. *World Neurosurg* 2015; 83: 80–86.
5) Umeda Y, Ishida F, Tsuji M, et al: [Computational fluid dynamics (CFD) analysis using porous media modeling predicts angiographic occlusion status after coiling of unruptured cerebral aneurysms - Preliminary study]. *JNET* 2015; 9: 69–77. (in Japanese)
6) Tsuji M, Ishikawa T, Ishida F, et al: Stagnation and complex flow in ruptured cerebral aneurysms: a possible association with hemostatic pattern. *J Neurosurg* 2017; 126: 1566–1572.
7) Boussel L, Rayz V, McCulloch C, et al: Aneurysm growth occurs at region of low wall shear stress: patient-specific correlation of hemodynamics and growth in a longitudinal study. *Stroke* 2008; 39: 2997–3002.
8) Yamamoto H, Kawamura K, Omura K, et al: Development of a compact-sized falling needle rheometer for measurement of flow properties of fresh human blood. *Int J Thermophysics* 2010; 31: 2361–2379.
9) Murray CD: The physiological principle of minimum work applied to the angle of branching of arteries. *J Gen Physiol* 1926; 9: 835–841.
10) Pries AR, Secomb TW, Gaehtgens P: Design principles of vascular beds. *Circ Res* 1995; 77: 1017–1023.
11) Sano T, Ishida F, Tsuji M, et al: Hemodynamic differences between ruptured and unruptured cerebral aneurysms simultaneously existing in the same location: 2 case reports and proposal of a novel parameter oscillatory velocity index. *World Neurosurg* 2017; 98: 868.e5–868.e10.
12) Hartert H: Flow properties of blood and other biological systems. Oxford, New York & Paris: Pergamon Press, 1960; 186–192.
13) Errill EW: Rheology of blood. *Physiol Rev* 1969; 49: 863–888.
14) Lowe GD, Fowkes FG, Dawes J, et al: Blood viscosity, fibrinogen, and activation of coagulation and leukocytes in peripheral arterial disease and the normal population in the Edinburgh Artery Study. *Circulation* 1993; 87: 1915–1920.
15) Velcheva I, Antonova N, Dimitrova V, et al: Plasma lipids and blood viscosity in patients with cerebrovascular disease. *Clin Hemorheol Microcirc* 2006; 35: 155–157.

16) Li RY, Cao ZG, Li Y, et al: Increased whole blood viscosity is associated with silent cerebral infarction. *Clin Hemorheol Microcirc* 2015; 59: 301–307.
17) Burger J, Yamamoto H, Suzuki T, et al: Application of falling-needle rheometry to highly concentrated DNA solutions. *Biorheology* 2014; 51: 29–45.
18) Ohta M, Wetzel SG, Dantan P, et al: Rheological changes after stenting of a cerebral aneurysm: a finite element modeling approach. *Cardiovasc Intervent Radiol* 2005; 28: 768–772.
19) Xiang J, Tremmel M, Kolega J, et al: Newtonian viscosity model could overestimate wall shear stress in intracranial aneurysm domes and underestimate rupture risk. *J Neurointerv Surg* 2012; 4: 351–357.
20) Suzuki T, Takao H, Suzuki T, et al: Variability of hemodynamic parameters using the common viscosity assumption in a computational fluid dynamics analysis of intracranial aneurysms. *Technol Health Care* 2017; 25: 37–47.